$^{11}B(\gamma, \pi^-)^{11}C$ cross section near threshold*

K. Min, P. Stoler, S. Trentalange, E. J. Winhold, and P. F. Yergin
Physics Department, Rensselaer Polytechnic Institute, Troy, New York 12181

A. M. Bernstein and W. Turchinetz
Physics Department and Laboratory for Nuclear Science, Massachusetts Institute of Technology, Cambridge, Massachusetts 02139

K. S. R. Sastry
Physics Department, University of Massachusetts, Amherst, Massachusetts 01002
(Received 18 June 1976)

Yields for the $^{11}B(\gamma,\pi^-)$ reaction have been measured between its threshold at 142.0 MeV and 169 MeV by observing the residual ^{11}C activity. The reaction was initiated by thin-radiator bremsstrahlung. Measurements were made in 1 MeV steps up to 150 MeV, and in larger steps above this. The present results are consistent with previous data for this reaction obtained at higher energies. The cross section values near threshold deduced from the data are compared to recent preliminary theoretical values.

[NUCLEAR REACTIONS $^{11}B(\gamma,\pi^-)$; bremsstrahlung end-point energies to 169 MeV; measured yields by residual activity; deduced $\sigma(E_\gamma)$ for $E_\gamma = E_{th}$ (142.0 MeV)–169 MeV.]

I. INTRODUCTION

Photopion production from a complex nucleus depends on: (1) the transition operator, (2) the nuclear wave functions, and (3) the pion-nucleus final state interaction. The threshold energy region is of special interest because the transition operator appropriate at these energies is expected[1] to have a simple form proportional to $\vec{\sigma}\cdot\vec{e}$, where $\vec{\sigma}$ is the nuclear spin operator and $\vec{e}$ is the photon polarization vector. In addition, pion reabsorption in the final state is less important than at higher energies. If these factors are sufficiently well understood, one can hope to use photopion production in the threshold region as a tool for studying nuclear properties.[2]

Experimental measurements of pion photoproduction suffer, however, from inherently low yields and relatively high backgrounds near threshold. When bremsstrahlung photons are used, it is the difference between two successive photopion yields which essentially determines the cross section. Therefore, threshold measurements are subject to very stringent requirements on data reproducibility and counting statistics. For this reason, most of the earlier experimental work on photopion production[3-7] did not provide any information near threshold. More recently, however, as higher intensity bremsstrahlung photons became available from new electron linear accelerators at Saclay and MIT, the first experimental measurements of threshold photopion cross sections have been reported.[8-11] In parallel with this development, more complete theoretical calculations[12-14] have also become available. In a recent experiment Deutsch *et al.*[8] measured the $^6Li(\gamma,\pi^+)$ cross section near threshold relative to the (γ,π^+) cross section for hydrogen, and found the ^6Li cross section to be only about 60% of the theoretical values calculated by Koch and Donnelly.[12,13] However, Tzara, in a later communication,[9] has indicated that further experiments using improved techniques have yielded higher cross sections. In addition, the extraction of the nuclear form factors from electron scattering has been reexamined,[15,16] with the result that the theoretical cross section values have been lowered by roughly 15%. Therefore, the discrepancy between theory and experiment in $^6Li(\gamma,\pi^+)$ appears to be less than was originally reported, and is within the combined experimental and theoretical uncertainties of about 20%.[9] In the case of $^{12}C(\gamma,\pi^-)$, the experimental value[11] for the cross section at threshold is consistent with theoretical calculations,[14] but rises somewhat more rapidly with energy than predicted theoretically.

It is of considerable interest to examine other cases, both (γ,π^+) and (γ,π^-), in those light nuclei for which the needed nuclear structure information is known. One such case is $^{11}B(\gamma,\pi^-)^{11}C$, and the present paper reports a measurement of the total cross section near threshold for this reaction by observing the residual ^{11}C activity. The reaction has been previously studied,[3,4,6,7,17] but the emphasis in the earlier experiments was on the general energy dependence of the cross section over a broad energy interval rather than on the de-

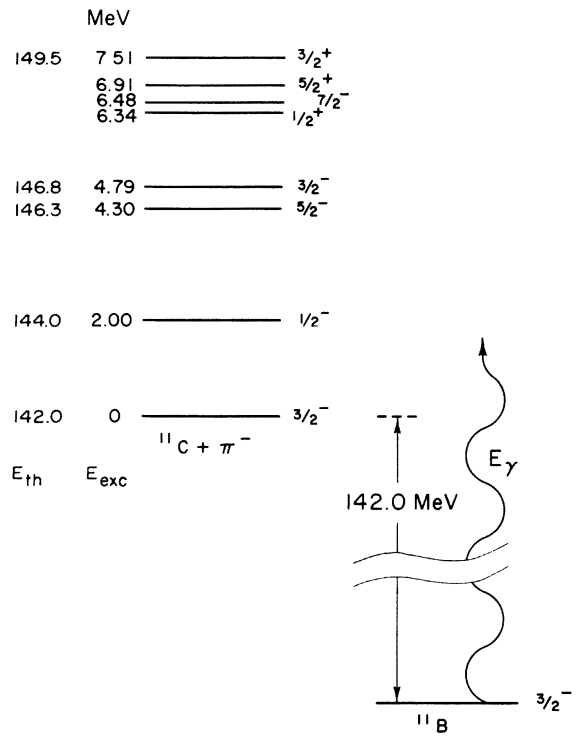

FIG. 1. Particle-stable states of ^{11}C accessible in the present $^{11}B(\gamma,\pi^-)$ experiment.

tails near threshold. The nucleus ^{11}B is an interesting one to study because the ^{11}C ground state is the mirror of the ^{11}B ground state and the first excited state in ^{11}C is at a relatively high excitation energy (2.0 MeV). As Fig. 1 indicates, the daughter nucleus ^{11}C has a limited number of accessible particle-stable excited states, and the four negative-parity excited states are well described[18] by intermediate-coupling wave functions with $1p$ configurations. The ^{11}C β^+ activity provides a convenient experimental signature for the reaction studied. Finally, several theoretical calculations[19-21] on $^{11}B(\gamma,\pi^-)^{11}C$ near threshold exist. Tzara[20] has examined the effect of Coulomb distortion of the pion wave function on the cross section near threshold. Recently Koch and Donnelly[21] have carried out preliminary calculations of the cross sections for threshold transitions to the ground and first excited states of ^{11}C, including both the nuclear and Coulomb distortion of the pion wave function.

II. EXPERIMENT

The experiment was performed at the MIT Bates linear accelerator. Yields were measured at bremsstrahlung end-point energies ranging from about 120 to 170 MeV. A special effort was made to measure the yields in detail, in energy steps of 1 MeV, at energies within 10 MeV of the threshold at 142.0 MeV.

In the experiment, the $^{11}B(\gamma,\pi^-)^{11}C$ yield from high purity boron samples was measured relative to the $^{12}C(\gamma,n)^{11}C$ yield from polyethylene monitor foils. This was done by observing the induced 20.4 min ^{11}C β^+ activity in both boron and polyethylene following bremsstrahlung irradiation. $^{12}C(\gamma,n)$ was used as the monitor reaction since it leads to the same residual activity as $^{11}B(\gamma,\pi^-)$, and its yield is known and varies slowly with energy at these energies.

The irradiation geometry is shown in Fig. 2. The electron beam from the Bates linac was delivered to the irradiation area with the beam switchyard slit system set to limit the fractional momentum width of the beam to 2.5×10^{-3}. The beam repetition rate was 60 Hz, pulse duration was 12 μs, and peak current typically 12 mA. Bremsstrahlung was produced when the electron beam passed through a tungsten radiator foil [0.014 radiation lengths (r.l.)], an aluminum vacuum window (0.004 r.l.) and a beryllium oxide viewing screen (0.001 r.l.). The emergent electron beam was then magnetically deflected into a shielded beam dump.

Three boron samples were used in the experiment, each being approximately cylindrical (about 0.95 cm in diameter and 1.27 cm long), of ultrahigh purity (99.9995%) polycrystalline boron.[22] At each energy each of the three samples was irradiated, in turn, for 30 min, together with two 0.0025 cm polyethylene monitor foils, which were cut to match the boron sample shape and were affixed to the front and rear faces of the sample.

In order to maximize reproducibility, the electron beam was centered in a nonintercepting position monitor located 60 cm upstream from the radiator, and the bremsstrahlung beam was kept in the same spatial position relative to the sample

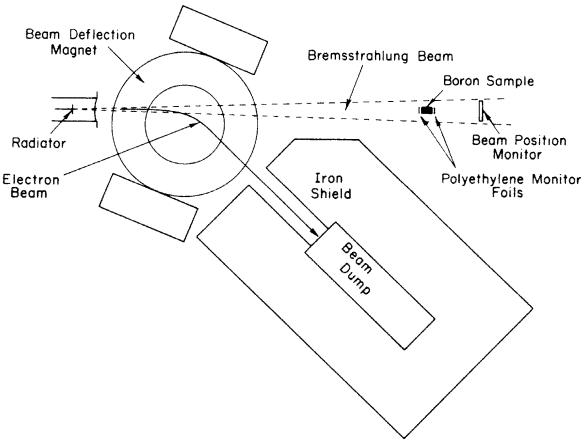

FIG. 2. Schematic plan of the irradiation geometry.

by centering it on a beam position monitor located about 30 cm downstream from the sample. The beam centering was further checked in each run by irradiating and counting a 19 cm square polyethylene sheet and comparing its activity to that of the small monitor foils. There was no need to compensate for variations of beam intensity with time during each run, since the same activity was measured in samples and monitors.

A set of four independent scintillation counter systems, each with a 7.62×7.62 cm crystal, was used for activity counting. Two counters were used for the boron samples and two for the polyethylene monitors. In each system a single channel analyzer selected those pulses corresponding to the 511 keV positron annihilation photon peak. A printing scaler system recorded the number of pulses received in successive 100 s intervals.

Counting the residual activity in the sample and monitor foils was started within a few minutes of the end of each irradiation. Each sample-monitor pair was counted first in one detector array ("early counters") for about $\frac{1}{2}$ h, then transferred to the other system ("late counters") and counted for another $\frac{1}{2}$ h. Every time the samples were moved, brief checks of electronic stability were made with standard ^{22}Na sources. Special care was taken to insure reproducibility of positioning of the samples relative to the detector. The absolute efficiency of each counter system for detecting the radiations from sample or monitors was determined using standard ^{22}Na sources in the same counter geometry, suitably averaging over the finite sample size and correcting for sample self-absorption.

III. DATA ANALYSIS AND RESULTS

The boron activity data were corrected for both time-independent background (typically 0.5% for the early counters) and for the 53.3 day 478 keV γ ray activity from photon-induced production of ^{7}Be in the boron sample (in the range from $\frac{1}{2}$% to 3% for the early counter data for most runs, with highest values for the later runs due to buildup of ^{7}Be in the boron samples). Counting losses due to system dead time and background corrections for ^{11}C activity produced in earlier runs were negligible. After these corrections, both boron and polyethylene decay data showed no deviation from the 20.4 min half-life characteristic of ^{11}C. The summed boron and polyethylene counts from each run were also corrected for small electronic drifts from run to run as determined by the ^{22}Na source checks (typically 0.3% for successive runs). The boron/carbon yield ratio R for each run was obtained from these values by correcting for the number of ^{11}B and ^{12}C nuclei in samples and monitors and for the sample- and monitor-detector efficiencies as experimentally determined. Separate R values were obtained from the early and late counter data for individual runs. Counting statistics were 0.25% for early counter data from a typical run and 0.4% for late counter data.

It was found that the variation in R values from different runs at the same energy was generally larger than counting statistics alone would produce and could not be accounted for by uncertainties in the ^{7}Be background correction. It thus appears that despite careful control of the irradiation and counting conditions there were one or more sources of significant uncontrolled variations in the experiment. One possible source of these variations may have involved fluctuations in the electron-beam intensity distribution, within the fixed-position beam spot on the bremsstrahlung radiator. The data are consistent with these additional random errors having constant variance throughout the experiment and contributing about 0.4% to the standard deviation of the mean for each three-sample set of R values from the early or late counter data. The spread of R values in the different three-sample sets is consistent with a value of 0.5% for the overall standard deviation of the mean for R from three-sample early counter data sets and 0.7% for sets of late counter data. We therefore used these values for the standard deviation of R for each three-sample set, and combined early and late counter R values to obtain weighted R values for each set of runs. These are plotted versus energy in Fig. 3, where R values from repeated run sets at a given energy have been combined.

The sizable R values below the ^{11}B photopion threshold at 142.0 MeV constitute a background whose magnitude and slow variation with energy are consistent with an origin in the two-step process in which the $^{11}B(\gamma,p)$ reaction produces protons which then, inside the boron sample, cause the $^{11}B(p,n)^{11}C$ reaction. Some contribution from carbon impurity in the boron sample via the $^{12}C(\gamma,n)^{11}C$ reaction, may also be present despite efforts to obtain samples with extremely low carbon content. The experiment is very sensitive to such impurities since the cross section for $^{12}C(\gamma,n)$ is much higher than the boron photopion cross section and is largest at energies (20–30 MeV) where the photon intensity in the bremsstrahlung beam is much larger than at the energies (140–150 MeV) used for the photopion reaction. To obtain the best estimate of the background from these sources underlying the data above the photopion threshold, the below-threshold data were fitted by a straight line using weighted least squares, and the line was extrapolated above threshold, as shown in Fig. 3.

Absolute $^{11}B(\gamma,\pi^-)$ yields were obtained by multi-

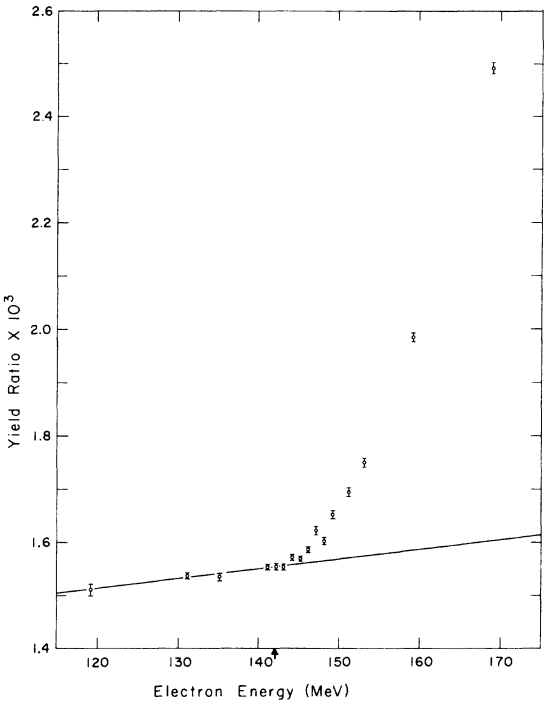

FIG. 3. The measured boron/carbon yield ratio R as a function of electron energy. Error bars on the points were determined as discussed in the text. The arrow indicates the location of the $^{11}B(\gamma,\pi^-)$ threshold. The solid straight line is a weighted least squares fit to the below-threshold background data points.

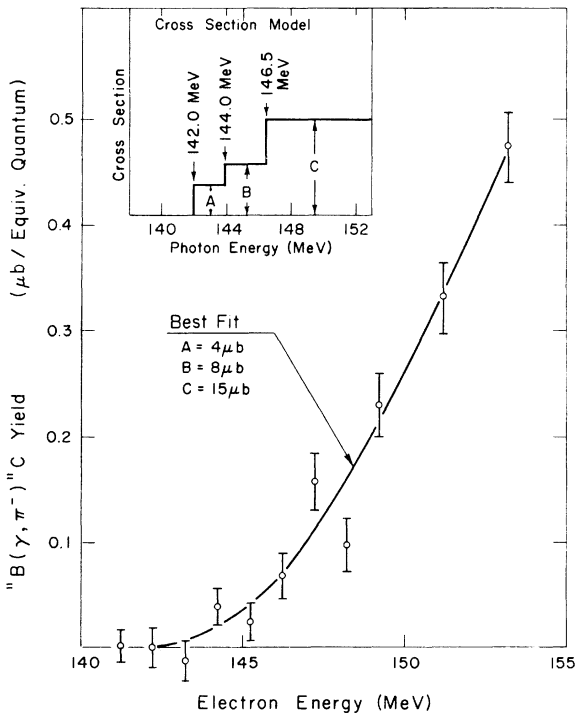

FIG. 4. Low-energy absolute $^{11}B(\gamma,\pi^-)$ yield data. The insert shows the three-step cross section model used to fit the data. The solid yield curve represents the best fit of this model to the data, and corresponds to $A = 4\,\mu$b, $B = 8\,\mu$b, and $C = 15\,\mu$b.

plying the background-subtracted net R values by the corresponding absolute yield for the reaction $^{12}C(\gamma,n)$. The latter was obtained by evaluating published values[23-27] and was taken to vary linearly from 2.70 mb per equivalent quantum at 140 MeV to 2.79 mb/Q at 170 MeV. The absolute accuracy of these values is probably about ±10%. The resultant net yield points near threshold are shown in Fig. 4. It can be seen that because of the large background subtraction the yield points near threshold have large fractional uncertainties, and therefore admit of a fairly broad range of yield curve fits and corresponding cross section values, especially within a few MeV of threshold.

The photopion yield $Y(T_0)$ obtained with bremsstrahlung photons at an electron energy T_0 is related to the photopion cross section $\sigma(k)$ via

$$Y(T_0) = C\int_{E_{th}}^{T_0} \sigma(k)N(k, T_0)dk\,, \tag{1}$$

where E_{th} is the threshold energy, $N(k,T_0)$ is the number of photons per unit energy of energy k incident on the sample, and C is a constant which includes sample-dependent factors. Various unfolding techniques[28,29] have been used to effectively solve this integral equation to obtain the cross section $\sigma(k)$. In a procedure which is straightforward in principle, the integral in (1) is approximated by a sum

$$Y_i(T_0) = C\sum_{j=1}^{i} N_{ij}\sigma_j\,, \tag{2}$$

where σ_j is the average value of $\sigma(k)$ in the jth photon energy interval and N_{ij} is the number of photons in the same interval with electron energy T_0. In matrix notation

$$\vec{Y} = N\cdot\vec{\sigma}\,, \tag{3}$$

where $\vec{Y}$ and $\vec{\sigma}$ are column matrices with elements Y_i and σ_i, and N is a square matrix with elements CN_{ij}. The solution of (3) is then

$$\vec{\sigma} = N^{-1}\cdot\vec{Y}\,. \tag{4}$$

Equation (4) can be used to directly extract cross sections from the higher energy yield data in the present experiment. However, the near-threshold yield values have uncertainties which are too large for a direct point-by-point unfolding using (4) to yield meaningful cross section values. Near threshold we have instead chosen to assume specific cross section shapes with a limited number

of adjustable parameters. Acceptable ranges of the parameters were obtained by using (2) to calculate yields corresponding to various cross section parameter values and using the χ^2 test to compare these computed yields with the experimental yield values.

The bremsstrahlung spectra $N(k, T_0)$ used throughout these calculations were obtained from the formulas of Matthews and Owens[30] which are based on the Bethe-Heitler theory with end-point shape corrections added, and which include effects of finite radiator thickness and incident electron energy spread. The spectrum took into account radiation from the tantalum radiator, the aluminum end window, and the beryllium oxide viewing screen. The end window and viewing screen together only accounted for about 11% of the total bremsstrahlung incident on the sample because of angle broadening of their radiation arising from the prior multiple electron scattering in the tantalum radiator.

We assumed a constant cross section of value A between 142.0 and 144.0 MeV and a constant cross section of value B between 144.0 and 146.5 MeV. As can be seen in Fig. 1, the thresholds for the first three excited states in ^{11}C are at 144.0, 146.3, and 146.8 MeV, so that the cross section A in the first interval is due only to ground state transitions, and the cross section B in the second interval is due essentially to ground and first excited state transitions. This assumption of an abrupt step in the cross section at the threshold for each final state is expected theoretically as a result of the interaction of the negative pion with the Coulomb field of the nucleus.[20] The assumption of a constant cross section to each state in the energy region near its threshold is taken to represent an average cross section near threshold.

The range of acceptable A and B cross section values resulting from a fit of this model to the five experimental points below 146.5 MeV is shown in Fig. 5, where the curves are constant χ^2 contours. The figure shows the expected strong correlation between A and B values.

In the energy range between 146.5 and 153.2 MeV, we have assumed a constant cross section of value C. We have determined the range of C values consistent with the yield data by making a three-parameter fit to the ten yield points up to 153.2 MeV, and the results are summarized in Fig. 6. As expected, the C values are correlated much less strongly with A and B than are A and B with each other. The calculated yield curve for the best three-parameter fit ($A = 4\,\mu$b, $B = 8\ \mu$b, $C = 15\ \mu$b) is plotted in Fig. 4 along with the experimental yield points.

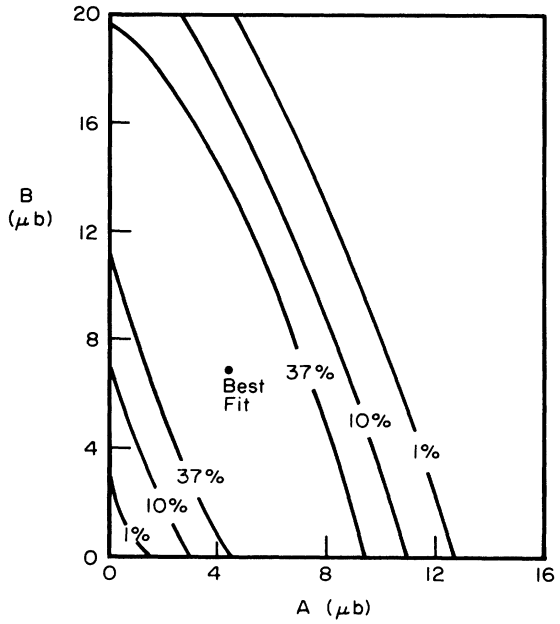

FIG. 5. Contours of constant χ^2 probability for fits of the experimental yield data below 146.5 MeV with a two-step cross section model (cross section A between 142.0 and 144.0 MeV, and cross section B between 144.0 and 146.5 MeV). The indicated percentage values on each contour are percentages of the χ^2 probability for the best fit to the yield data.

If the three-step model (parameters A, B, and C) is fitted to the ten yield points up to 153.2 MeV, and the additional physically plausible restriction that $A \leq B \leq C$ is made, the uncertainties in A and B are decreased from those shown in Fig. 5, and are given in Fig. 7. The best-fit A and B values are not significantly different from the earlier values. The requirement $A \leq B \leq C$ is consistent with theoretical expectations of a positive step in the cross section at the onset of each new final state and a positive cross section slope between steps.

To see how much these results for A and B depend on the assumption of a constant C cross section in the energy range 146.5–153.2 MeV, the three-parameter fit of the data up to 153.2 MeV was repeated assuming that the cross section in the C region had a constant positive slope. The overall quality of fit varies little for C slope values ranging from 0 to 2.5 μb/MeV. The best-fit value for A remains between 4 and 5 μb and that for B between 8 and 10 μb for this range of C slopes, and their uncertainties do not vary significantly from those shown in Fig. 7 for zero C slope. In addition, the best-fit cross section value at the midpoint of the C interval ($E = 149.85$ MeV) remains near 15 μb (between 14.9 and 16.3 μb)

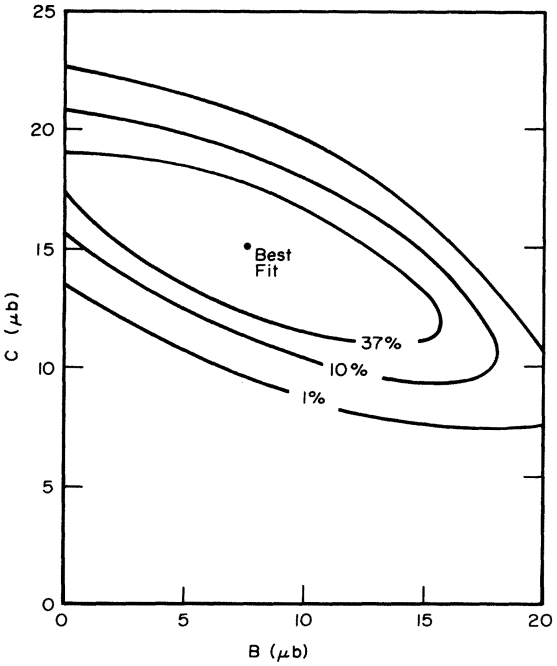

FIG. 6. Contours of constant χ^2 probability for fits of the experimental yield data below 153.2 MeV with the three-step cross section model shown in Fig. 4. The contours represent projections on the BC plane of surfaces of constant probability in ABC space. The indicated percentage values on each contour are percentages of the χ^2 probability for the best fit to the yield data.

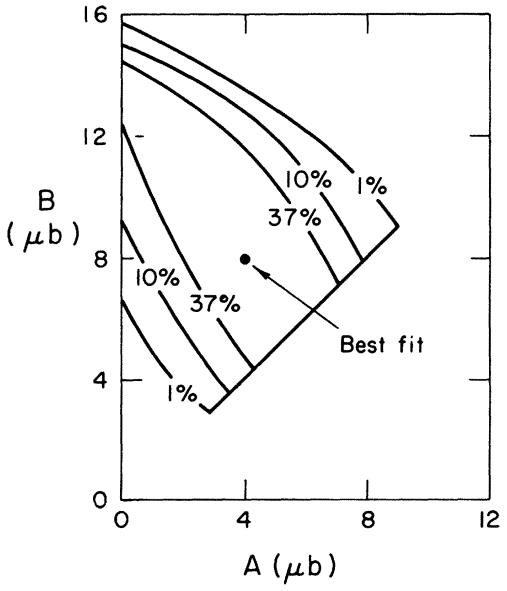

FIG. 7. See caption for Fig. 6. The contours represent projections on the AB plane of surfaces of constant probability in ABC space under the requirement that $A \leq B \leq C$.

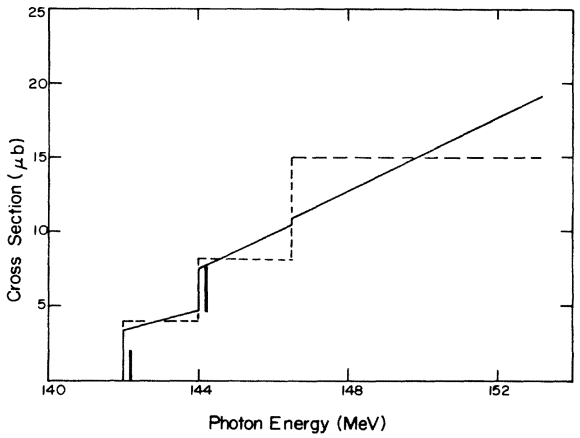

FIG. 8. The solid curve is the best-fit three-step cross section taking the same slope per unit height as that measured (Ref. 11) for the $^{12}C(\gamma,\pi^-)$ ground state transition. The vertical bars are the preliminary theoretical results of Koch and Donnelly (Ref. 21). The dashed curve is the best-fit three-step cross section with horizontal steps.

over this range of slopes.

If the A and B regions are also permitted to have positive slopes, the quality of fit for the three-step model is effectively unchanged from the zero slope case provided the cross section values at the midpoints of the A and B regions are kept equal to their zero slope values. This is true for the full range of slopes for which the cross section steps remain positive. Figure 8 shows the best-fit three-step cross section resulting from assuming the same slope per unit step height for each step as that experimentally measured[11] for the $^{12}C(\gamma,\pi^-)$ ground state transition.

There are two additional experimental yield points above 153.2 MeV which were not included in the above analysis. Because the yield is rapidly rising with energy in this energy region, it is possible to perform a direct unfolding using (4) to obtain average cross section values for the energy regions between 153.2 and 159.2 MeV, and between 159.2 and 169.2 MeV. This involves in effect fitting one parameter (the cross section value) to each data point. The cross sections thus obtained are shown in Fig. 9 together with the best-fit lower energy cross section curve of Fig. 8. As Eq. (4) indicates, these two higher energy cross section values depend on all lower energy yield values, but they do not depend on any assumptions made in extracting the lower energy cross section values (A, B, and C), nor do the lower energy cross section values depend at all on the cross section values assigned to these two higher energy points.

The effects of electron beam energy scale uncertainties, estimated to be ±300 keV, have not

been included in the above analysis. The parameters A and B are particularly sensitive to energy scale shifts; a 300 keV scale shift will raise or lower both A and B by about 0.7 μb.

IV. DISCUSSION

Along with the recently reported $^{12}C(\gamma,\pi^-)$ measurement, this experiment represents the first attempt to measure the (γ,π^-) cross section for a complex nucleus at energies within 10 MeV of threshold. The $^{11}B(\gamma,\pi^-)$ reaction has however been previously studied experimentally at energies of 160 MeV and above.[3,4,6,7,17] The earlier results below 185 MeV are displayed in Fig. 9. It appears that there is satisfactory agreement in cross section values between our highest energy points and these previous measurements.

Of greater interest is a comparison of the present cross section values near threshold with theoretical predictions. Unfortunately, complete calculations of the cross section to the several low-lying states in ^{11}C as a function of energy in the threshold region have not yet been performed. Koch and Donnelly[21] have made preliminary calculations of the $^{11}B(\gamma,\pi^-)$ cross section at threshold leading to the ground and first excited states of ^{11}C, using the same procedure as with their earlier calculations[12,13] of ^6Li and ^{12}C. These calculations include both nuclear and Coulomb distortion of the outgoing pion wave function but are restricted to s-wave pions. They obtain a value for the threshold cross section step of about 2 μb for the ground state of ^{11}C and a value of about 3 μb for the threshold step in the cross section to the first excited state. These values are shown as the vertical bars on Fig. 8. When the uncertainties in the present experimental cross section data as given in Fig. 7 are taken into account, it is evident that there is no significant disagreement between experiment and theory.

The cross section to the second excited and higher states has not been calculated by Koch and Donnelly. These states were included, however, in the plane wave calculation at 160 MeV by Janecek,[31] who found significant strength only to the first three excited states, but with an overall cross section to all three comparable to the ground state cross section. Calculations of the cross sections to the higher excited states in the threshold region are needed.

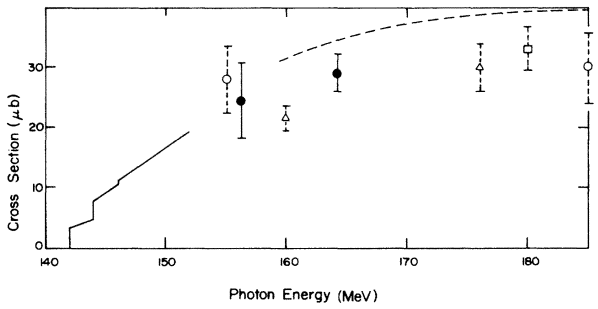

FIG. 9. The solid line and solid points are the present cross section results. The two open circle points are the results of Hughes and March (Ref. 3), the two open triangle points are the results of Dyal and Hummel (Ref. 4), the dashed curve is from the work of Nydahl and Forkman (Ref. 6), while the open square point is due to Noga *et al*. (Ref. 7).

ACKNOWLEDGMENTS

We thank E. C. Booth, B. C. Chasan, L. J. McVay, H. A. Medicus, A. Levin, S. E. Morrissey, J. J. Napolitano, P. Pella, D. Rowley, and R. Smalley for their contributions to this experiment. J. L. Matthews very kindly provided us with her bremsstrahlung spectrum codes. We thank P. T. Demos and the Bates laboratory staff for their helpful efforts. The accelerator staff was most helpful in obtaining satisfactory beams under difficult accelerator shakedown conditions. Finally, we thank J. H. Koch and T. W. Donnelly for providing us with the preliminary results of their theoretical calculations.

*Supported in part by the National Science Foundation under Grant No. MPS73-04979 A01 and by the U. S. Energy Research and Development Administration under Contract No. E(11-1)-3039.

[1]M. Ericson and M. Rho, Phys. Rep. 5, 58 (1972).
[2]See e.g. H. Überall, B. A. Lamers, C. W. Lucas, and A. Nagl, Phys. Lett. 44B, 324 (1973).
[3]I. S. Hughes and P. V. March, Proc. Phys. Soc. (London) 72, 259 (1958).
[4]P. Dyal and J. P. Hummel, Phys. Rev. 127, 2217 (1962).
[5]R. A. Meyer, W. B. Walter, and J. P. Hummel, Phys. Rev. 138, B1421 (1965).
[6]G. Nydahl and B. Forkman, Nucl. Phys. B7, 97 (1968).
[7]V. I. Noga, Yu N. Ranyuk, P. V. Sorokin, and B. A. Tkachenko, Yad. Fiz. 14, 904 (1971) [Sov. J. Nucl. Phys. 14, 506 (1972)].
[8]J. Deutsch, D. Favart, R. Prieels, B. Van Ostaeyen, G. Audit, N. de Botton, J. L. Faure, Cl. Schuhl, G. Tamas, and C. Tzara, Phys. Rev. Lett. 33, 316 (1974).
[9]C. Tzara, in Proceedings of the International Topical Conference on Meson-Nuclear Physics, Pittsburgh, Pennsylvania, 1976 (unpublished).

[10]P. F. Yergin, L. McVay, K. Min, P. Pella, D. Rowley, P. Stoler, S. Trentalange, E. J. Winhold, K. S. R. Sastry, and W. Turchinetz, Bull. Am. Phys. Soc. 20, 661 (1975).
[11]A. M. Bernstein, N. Paras, W. Turchinetz, B. Chasan, and E. C. Booth, Phys. Rev. Lett. (to be published).
[12]J. H. Koch and T. W. Donnelly, Nucl. Phys. B64, 478 (1973).
[13]J. H. Koch and T. W. Donnelly, Phys. Rev. C 10, 2618 (1974).
[14]A. Nagl, F. Cannata, and H. Überall, Phys. Rev. C 12, 1586 (1975); A. Nagl and H. Überall (private communication).
[15]J. C. Bergstrom, I. P. Auer, and R. S. Hicks, Nucl. Phys. A251, 401 (1975).
[16]J. B. Cammarata and T. W. Donnelly (unpublished).
[17]I. Blomqvist, G. Nydahl, and B. Forkman, Nucl. Phys. A162, 193 (1971).
[18]S. Cohen and D. Kurath, Nucl. Phys. 73, 1 (1965).
[19]D. Griffiths and C. W. Kim, Nucl. Phys. B6, 49 (1968).
[20]C. Tzara, Nucl. Phys. B18, 246 (1970).
[21]J. H. Koch and T. W. Donnelly (private communication).
[22]Supplied by Eagle-Picher Industries, Inc., Miami Research Labs, Miami, Oklahoma 74354.
[23]W. C. Barber, W. D. George, and D. D. Reagan, Phys. Rev. 98, 73 (1955).
[24]A. Masaike, J. Phys. Soc. Jpn. 19, 427 (1964).
[25]V. di Napoli, F. Dobici, O. Forina, F. Salvetti, and H. G. de Carvalho, Nuovo Cimento 55B, 95 (1968).
[26]Yu. P. Antuf'ev, I. I. Miroshnichenko, V. I. Noga, and P. V. Sorokin, Yad. Fiz. 6, 431 (1967) [Sov. J. Nucl. Phys. 6, 312 (1968)].
[27]G. Hyltén, Nucl. Phys. A158, 225 (1970).
[28]A. S. Penfold and J. E. Leiss, Phys. Rev. 114, 1332 (1959).
[29]B. C. Cook, Nucl. Instrum. Methods 24, 256 (1963).
[30]J. L. Matthews and R. O. Owens, Nucl. Instrum. Methods 111, 157 (1973).
[31]P. Janeček, Phys. Scr. 7, 141 (1973).